Available online at www.sciencedirect.com

SciVerse ScienceDirect

Ceramics International 38 (2012) 1325–1330

CERAMICS INTERNATIONAL

www.elsevier.com/locate/ceramint

Preparation and characterization of hydroxyapatite–forsterite–bioactive glass nanocomposite coatings for biomedical applications

M. Mazrooei Sebdani *, M.H. Fathi

Biomaterials Group, Department of Materials Engineering, Isfahan University of Technology, Isfahan, 84156-83111, Iran

Received 18 April 2011; received in revised form 23 August 2011; accepted 1 September 2011
Available online 8 September 2011

Abstract

In order to improve biological and mechanical properties of hydroxyapatite, the concept of hydroxyapatite-included nanocomposite coatings was introduced. By judiciously choosing constituent ceramics for composites preparation, the biological and mechanical performance of coatings can be tailored in order to meet various clinical requirements. The aim of this work was fabrication, development and characterization of novel hydroxyapatite–forsterite–bioactive glass nanocomposite coatings. The sol–gel technique was used to prepare hydroxyapatite–forsterite–bioactive glass nanocomposite in order to apply coating on 316L stainless steel (SS) by dip coating technique. The X-ray diffraction (XRD), scanning electron microscopy (SEM) and energy dispersive X-ray analysis (EDX) were used to investigate the phase structure, microstructure and morphology of the coating. In order to evaluate the forsterite incorporation influence upon bioactivity, the changes on the surfaces of the prepared composite coatings after the predicted days of contact with simulated body fluid (SBF) were investigated by SEM. Results showed that the suitable calcined temperature for nanocomposite coatings with different amounts of forsterite was 600 °C. At this temperature, the homogenous and crack-free coating could attach to the 316L SS substrate. The crystallite sizes of the prepared coatings were lower than 100 nm. The EDX analysis of hydroxyapatite–forsterite–bioglass, coated 316L SS surface, indicated consisting elements of prepared coatings and the substrate. During immersion in the SBF at pre-determined time intervals, apatite layer was formed and stimulation for apatite formation was increased with increase in forsterite amounts. It seems that hydroxyapatite–forsterite–bioactive glass nanocomposite coatings might be good candidates for biomedical applications.

© 2011 Elsevier Ltd and Techna Group S.r.l. All rights reserved.

Keywords: Sol–gel processses; Nanocomposite; Biomedical applications

1. Introduction

Bioceramics have been widely in use in medicine and dentistry. One remarkable success of these bioceramics is perhaps the emergence and clinical use of bioactive ceramics. These bioceramics include calcium phosphates, bioglass, A–W glass-ceramic, and other bioactive glasses and glass-ceramics that show a particular biological response at the interface of the material. Different phases of calcium phosphate ceramics can be used in medicine, depending on whether a bioactive or a resorbable material is desired. Among which, there is always a concern about hydroxyapatite (being the prominent family member) due to its closed resemblance to bones and teeth [1,2]. Different types of clinical applications of hydroxyapatite involve repair of bone defects, bone augmentation, as well as coatings for human body metallic implants [3]. However, poor mechanical properties of hydroxyapatite such as inherent brittleness, poor fatigue resistance and strength are the major limiting factors for load bearing applications [4]. Hence, a great deal of research has been carried out to improve the mechanical properties of hydroxyapatite [5]. The interest in this group of materials is for their use as a porous structure [6,7], as a bioactive phase in composites [8,9], and as a bioactive coating on metallic implants [10–12]. So, the concept of composite coatings including hydroxyapatite as a matrix and other ceramics as reinforcements was introduced. By judiciously choosing constituent ceramics of composites, the biological and mechanical performance of ceramic composites can be tailored in order to meet various clinical requirements [8,9,13–16]. So, a variety of ceramics has been investigated [17–20]. Ding studied a series of HA/BG composite coatings on titanium alloy substrate [17]. Fu used yttria-stabilized zirconia to

* Corresponding author. Tel.: +98 311 3912750; fax: +98 311 3912752.
E-mail address: m.mazrooei@ma.iut.ac.ir (M.M. Sebdani).

0272-8842/$36.00 © 2011 Elsevier Ltd and Techna Group S.r.l. All rights reserved.
doi:10.1016/j.ceramint.2011.09.008

reinforce hydroxyapatite coatings [18]. The certain composition of bioactive glasses containing CaO–SiO2–P2O5 could be potentially used as an additive for improving the properties of hydroxyapatite coating. These bioactive glasses show noticeable bioactivity performance. These bioactive glasses bond to both soft and hard tissues without an intervening fibrous layer [21]. Therefore, composite implants made of bioceramics such as HA and bioglass can form a strong bond with the host tissue resulting in their integration into the biological system [22]. On the other hand, such composites are not strong enough to be used for load bearing applications. Results show that compared with the monolithic matrix behavior the presence of this additive causes no considerable improvements in mechanical properties [23]. Thus, an optimization of the mechanical properties by a suitable choice of a ceramic reinforcement was needed. Forsterite could be an interesting material due to its better mechanical properties than hydroxyapatite and bioactive glass. In comparison with hydroxyapatite and bioglass, forsterite ceramics show considerable fracture toughness and hardness. The fracture toughness of forsterite ceramics is 2.4 $MPam^{1/2}$ superior to the lower limits reported for bone implants and hydroxyapatite ceramics (0.6–1 $MPam^{1/2}$) [24]. On the other hand, the addition of these ceramics, with reduced grain size lower than 100 nm, improves the properties of the composite coatings including them [25]. So, it is expected that compared with the monolithic matrix behavior, these nanocomposite coatings have better bioactivity and mechanical properties.

There are various methods of applying coatings. Coating application by a sol–gel technique is a promising alternative due to its suitable properties such as availability, commercial technique and ability to produce thin coating [26]. At this method, precursors are mixed at the molecular level [27].

The aim of this work was preparation and characterization of a novel hydroxyapatite–forsterite–bioactive glass nanocomposite coating via the sol–gel and dip coating methods.

2. Materials and methods

2.1. Preparation and characterization of the coating samples

The phosphoric pentoxide (P_2O_5, Merck), calcium nitrate tetrahydrate ($Ca(NO_3)_2{\cdot}4H_2O$, Merck), ethanol (Merck, 99.9% purity), forsterite nanopowder [28] and 45S bioactive glass nanopowder (45% SiO_2, 9% P_2O_5, 46% CaO) [29] were used to prepare nanocomposite coating and 20mm × 10mm × 2 mm of stainless steel plates (SS 316L) were selected as substrates. The phosphoric pentoxide (P_2O_5, Merck), calcium nitrate tetrahydrate ($Ca(NO_3)_2{\cdot}4H_2O$, Merck) and ethanol (Merck, 99.9%purity) were used to make hydroxyapatite sol. The preparation of the hydroxyapatite sol was described in detail elsewhere in the literature [4]. Hydroxyapatite–forsterite–bioactive glass nanocomposite coatings were prepared by adding bioactive glass nanopowder with 10 wt% and forsterite nanopowder with different amounts (0 wt% named F0, 10 wt% named F1, 20 wt% named F2, 30 wt% named F3) as reinforcements into the hydroxyapatite sol. Prior to coating via the sol–gel method, 20mm × 10mm × 2 mm of stainless steel plates (SS 316L) were polished to grade #1200 and then cleaned in an ultrasonic bath. After that, dip coating method was used and the 316L stainless steel samples were dipped into and withdrawn from the sol at a rate of 5 cm/min. The coated substrate underwent aging at ambient temperature and drying at 60 °C into the oven. Then, the prepared samples heated at different temperatures in order to determine the optimum temperature and to obtain different hydroxyapatite–forsterite–bioactive glass nanocomposite coating samples.

2.2. Characterization of the hydroxyapatite–forsterite–bioactive glass nanocomposite coatings

Phases of the prepared nanocomposite coatings were analyzed by an X-ray diffractometer (XRD, Philips X'Pert-MPD) with CuKα radiation at 40 kV and 30 mA, scanning in the standard θ to 2θ geometry from 20° to 80° at step size of 0.05° s^{-1}. The crystallite sizes of the prepared coatings were measured by XRD peak broadening and calculated using Scherer equation (1) [30]:

$$\beta = \frac{0.89\lambda}{t\cos\theta} \quad (1)$$

where β is the width of peak in the middle of its height, λ is the wavelength (=0.154 nm), θ is the Bragg angle and t is the apparent crystallite size. The crystallinity of the prepared composite coatings could be determined by the following Eq. (2) [31]:

$$X_C = 1 - \frac{V_{112/300}}{I_{300}} \quad (2)$$

where $V_{1\,1\,2/3\,0\,0}$ is the intensity of the hollow between (1 1 2) and (3 0 0) diffraction peaks of hydroxyapatite and $I_{3\,0\,0}$ is the intensity of (3 0 0) diffraction peak.

The morphology and microchemistry of the coatings were studied and evaluated by a scanning electron microscopy (SEM, Phillips XL30) equipped with energy dispersive spectroscopy (EDX, Seron AIS-2100) system. The cross sections of prepared coatings were observed using a SEM system.

2.3. In vitro bioactivity evaluation

The prepared coatings were submerged in the simulated body fluid (SBF) solution for characterizing the forsterite incorporation influence upon bioactivity. The changes on the surfaces of the composite coatings at pre-determined time intervals of contact with the SBF were investigated by soaking prepared nanocomposite coatings in the SBF without refreshing the soaking medium. The SBF was prepared according to the procedure described by Kokubo and Takadama [32]. The surface morphological changes of prepared coatings were analyzed after the immersion at predetermined time intervals (0–28 days). Scanning electron microscopy (SEM, Phillips XL30) was used to study the morphology changes that occurred in the coatings after the immersion in the SBF.

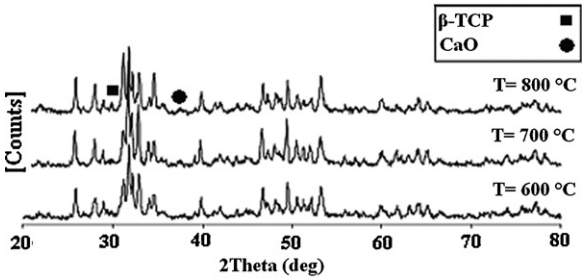

Fig. 1. X-ray diffraction patterns of a prepared composite coating with 10 wt% of forsterite calcined at different temperatures.

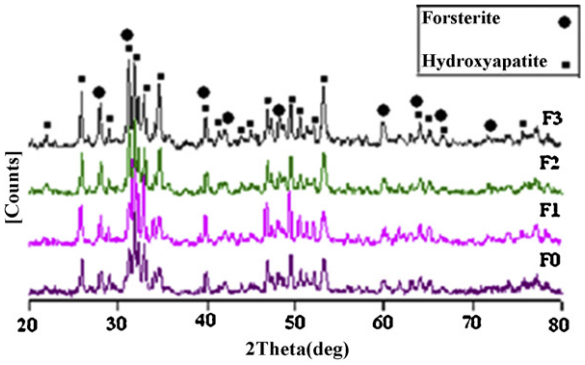

Fig. 2. X-ray diffraction patterns of prepared composite coatings. F0, without forsterite; F1, with 10 wt% forsterite; F2, with 20 wt% forsterite; F3, with 30 wt% forsterite.

Table 1
The amounts of crystallinity of the composite coatings with 10 wt% of forsterite post heat treated at different temperatures.

Crystallinity	Temperature
56%	600 °C
65%	700 °C
71%	800 °C

Table 2
The crystallite sizes of the prepared composite coatings with different amounts of forsterite.

Crystallite size	Sample
21 nm	F0
23 nm	F1
37 nm	F2
53 nm	F3

Composite coating: F0, without forsterite; F1, with 10 wt% forsterite; F2, with 20 wt% forsterite; F3, with 30 wt% forsterite.

3. Results and discussions

3.1. XRD analysis

Fig. 1 shows XRD patterns of prepared composite coatings with 10 wt% of forsterite at different temperatures. According to XRD patterns, the post heat treatment induced the phase transformation in the coatings. Post treatment could induce the transformation of hydroxyapatite into additional phases (β-TCP, CaO). As shown, hydroxyapatite decomposes into the additional crystalline phases (β-TCP and CaO) with increasing the sintering temperature to 700 °C and above. Therefore, the desired temperature was determined to be 600 °C. The suggested reaction is:

$$Ca_{10}(PO_4)_6(OH)_2 = 3Ca_3(PO_4)_2 + CaO + H_2O \quad (3)$$

The amounts of crystallinity of prepared composite coatings were calculated based on Eq. (2) and shown in Table 1. The higher the temperature of post heat treatment was, the higher the crystallinity was. The results showed that the coatings treated at 800 °C (the highest temperature used in this study) had the highest crystallinity. Fig. 2 shows XRD patterns of prepared composite coatings with different amounts of forsterite on the 316L SS substrate after heat treatment at 600 °C. As shown in these patterns, typical peaks matching JCPDS No. 09-0432 [33] and No. 34-0189 [34] files of hydroxyapatite and forsterite respectively were observed. The peak intensity of forsterite appeared to increase with increasing forsterite content, but the difference was minimal. The crystallite sizes of the prepared coatings with different amounts of forsterite calculated based on Eq. (1) were shown in Table 2. As it can be observed, the crystallite sizes of the prepared coatings were lower than 100 nm.

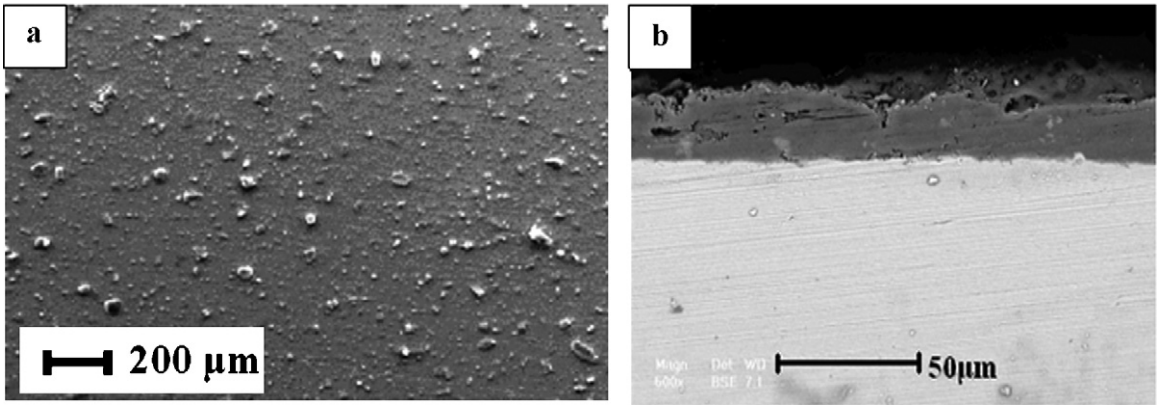

Fig. 3. SEM micrograph of (a) hydroxyapatite–forsterite–bioglass nanocomposite coating, (b) a cross-section view of the prepared nanocomposite coating with 10 wt% forsterite on the 316 L SS substrate that was calcined at 600 °C.

3.2. SEM evaluation and EDX analysis

The surface morphology of the prepared coating with 10 wt% forsterite that was calcined at 600 °C, was observed with SEM, and is shown in Fig. 3(a). The prepared coating revealed a smooth and fine surface without cracks (SEM micrograph of Fig. 3(a)). Such feature suggests a good potential for preparing efficient implant coatings in order to promote the osteointegration phenomenon. The cross-sectional morphology of the prepared composite coating with 10 wt% forsterite is shown in Fig. 3(b). A smooth, uniform, approximately 25–30 μm thick layer coating was formed on the 316L SS substrate.

The result of prepared typical coating composition analysis using EDX is shown in Fig. 4. The peaks of O, Si, P and Ca belong to the consisting elements of prepared coating and the peaks of Fe, Cr and Ni belong to 316 L SS.

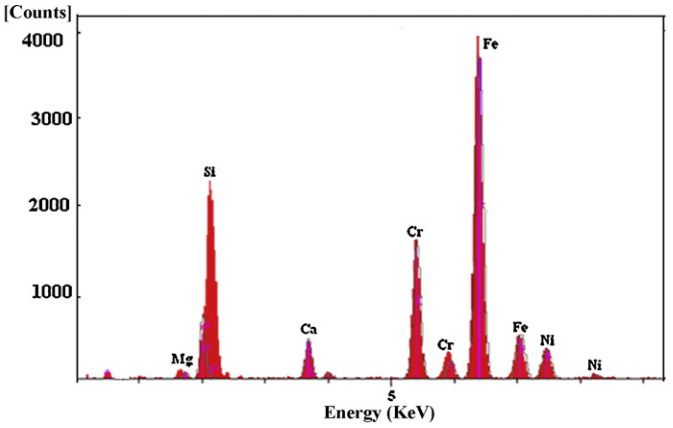

Fig. 4. Energy dispersive X-ray analysis (EDX) of the typical hydroxyapatite–forsterite–bioactive glass coated 316L SS sample.

3.3. In vitro bioactivity evaluation of prepared composite coatings

Hydroxyapatite–forsterite–bioglass nanocomposite coatings with different amounts of forsterite were immersed in the SBF under the physiological condition of pH 7.4 at 37.4 ± 0.1 °C for a period of 1–4 weeks for in vitro evaluations. Fig. 5; sections (A–D) show that the apatite layer precipitated on the prepared nanocomposite coatings with different amounts of forsterite after soaking in the SBF for 14 days. As shown, the growth of apatite layer for nanocomposite coatings with different amounts of forsterite differed markedly from another. It is clear to see that surface layer grows thicker with increase in forsterite amounts. Fig. 6; sections (A–D) show the surface

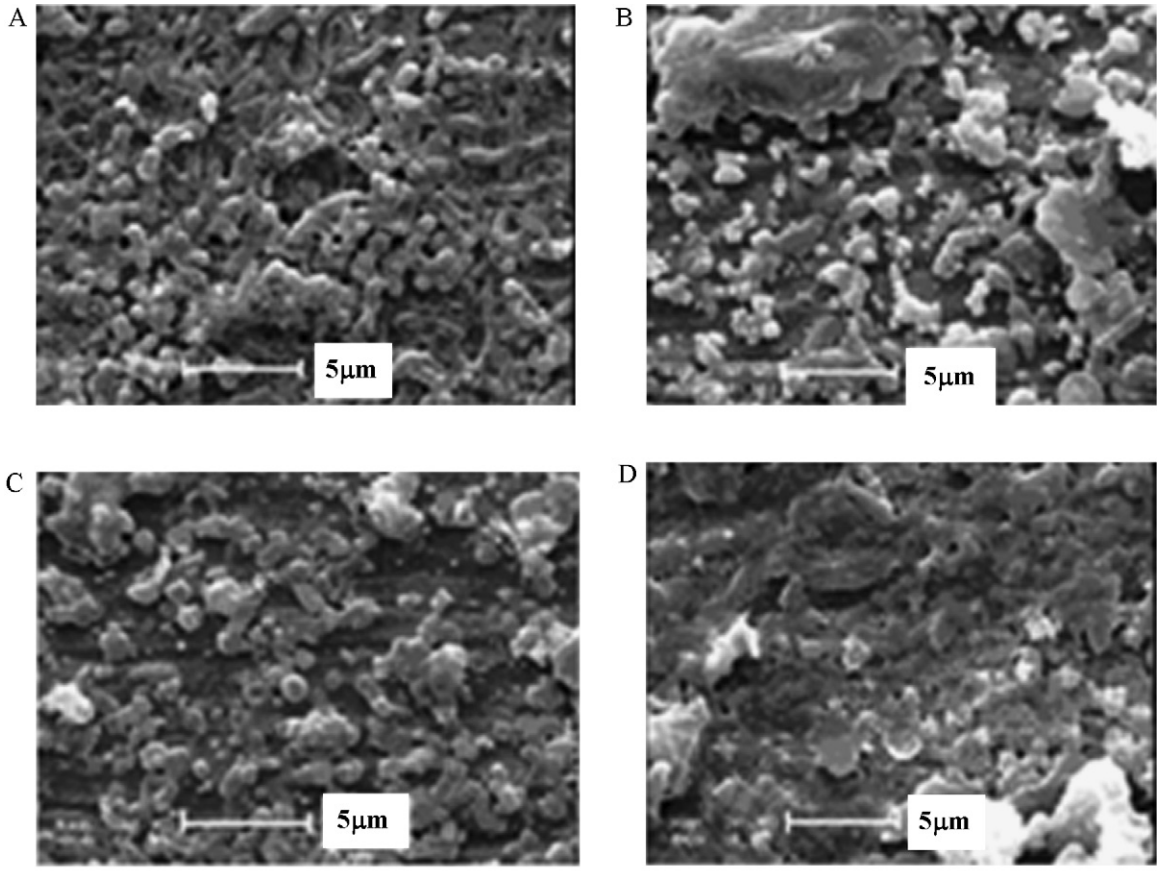

Fig. 5. SEM photograph of the different types of composite coatings (A) F0, (B) F1, (C) F2 and (D) F3 after immersion in the SBF solution for 14 days (F0, without forsterite; F1, with 10 wt% forsterite; F2, with 20 wt% forsterite; F3, with 30 wt% forsterite).

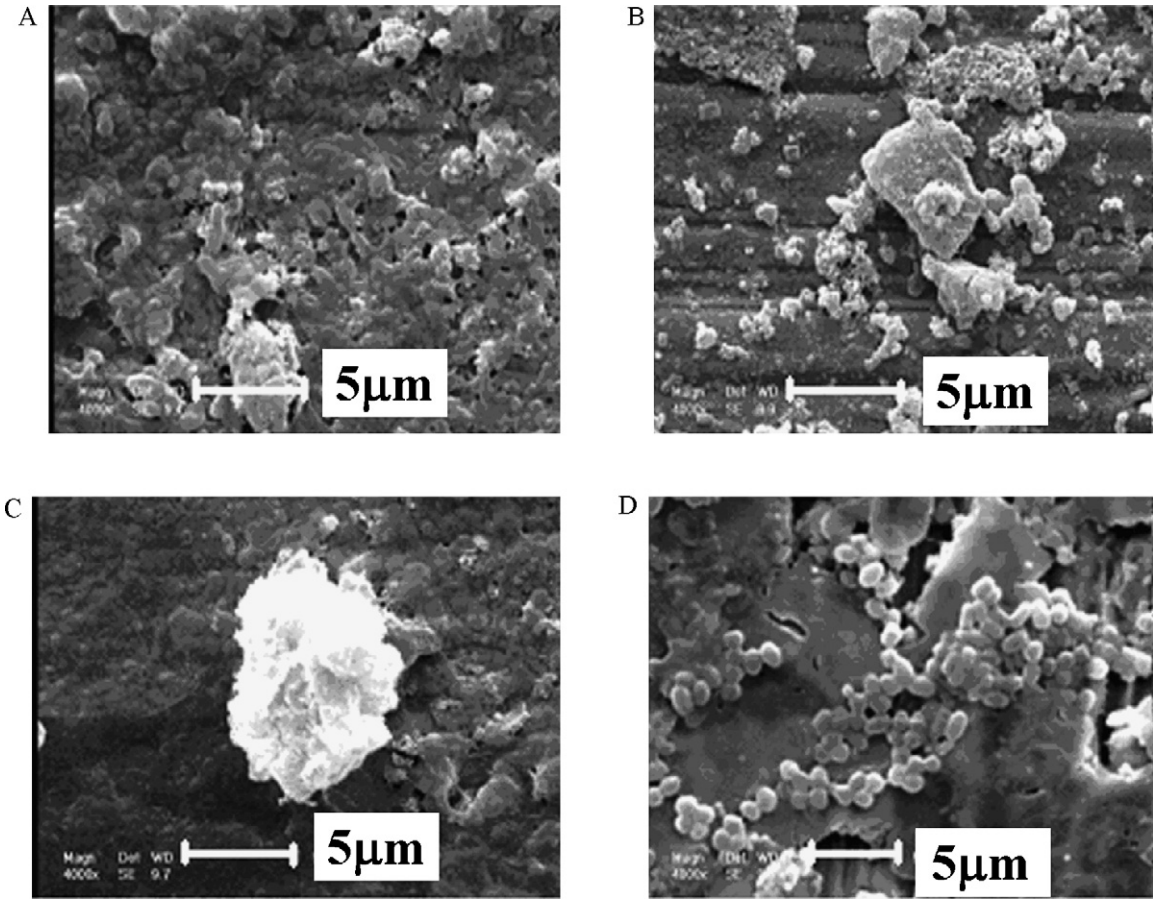

Fig. 6. SEM photograph of the different types of composite coatings (A) F0, (B) F1, (C) F2 and (D) F3 after immersion in the SBF solution for 28 days (F0, without forsterite; F1, with 10 wt% forsterite; F2, with 20 wt% forsterite; F3, with 30 wt% forsterite).

morphologies of the prepared coatings with different amounts of forsterite after soaking in the SBF for 28 days. The trend of increasing of apatite formation with increase in the forsterite amounts was also observed in Fig. 6. As comparison with Fig. 5 sections (A–D), Fig. 6 sections (A–D) show the greater formation of apatite as the length of the incubation period increased. It was noticed that the surface of the prepared coatings tested in vitro in the SBF for 28 days was covered to crystallites (Fig. 6 sections (A–D)). These clear topographic changes suggest that chemical ingrowths of calcium phosphate types occurred; In fact, it demonstrates the bioactive potential of the prepared coatings.

4. Conclusion

Novel hydroxyapatite–forsterite–bioactive glass composite coatings were successfully prepared by a sol–gel method. The suitable temperature for calcination of these nanocomposite coatings was 600 °C. At this temperature, the homogenous and crack-free coating could attach to the 316L SS substrate. Crystallite sizes of prepared coatings were lower than 100 nm. During immersion in the SBF, the apatite layer precipitated on the prepared nanocomposite coatings with different amounts of forsterite. Also, the trend of increasing of apatite formation with increase in forsterite amounts was observed. Results elicit that hydroxyapatite–forsterite–bioactive glass nanocomposite coatings with different amounts of forsterite might be good candidates for biomedical applications due to improved properties.

Acknowledgements

The authors thank for support of this research by Isfahan University of Technology.

References

[1] L.L. Hench, Bioceramics: from concept to clinic, J.Am. Ceram. Soc. 74 (1991) 1487–1510.
[2] F.H. Albee, H.F. Morrison, Studies in bone growth: triple calcium phosphate as a stimulus to osteogenesis, Ann. Surg. 71 (1920) 32.
[3] L.L. Hench, J. Wilson, An Introduction to Bioceramics, World Scientific, Singapore, 1993.
[4] M.H. Fathi, A. Hanifi, Evaluation and characterization of nanostructure hydroxyapatite powder prepared by simple sol–gel method, Mater. Lett. 61 (2007) 3978–3983.
[5] G. Göller, H. Demirkıran, F.N. Oktar, E. Demirkesen, Processing and characterization of bioglass reinforced hydroxyapatite composites, Ceram. Int. 29 (2003) 721–724.
[6] H.Y. Yang, M. Wang, Investigation into manufacture of porous hydroxyapatite via. three different routes and effects of porosifiers, Bioceramics 12 (1999) 349–352.

[7] C.X. Wang, M. Wang, Fabrication and characterisation of porous tricalcium phosphate, in: Proceedings of the 10th International Conference on Biomedical Engineering, Singapore, (2000), pp. 547–548.
[8] M. Wang, D. Porter, W. Bonfield, Processing, Characterisation, and evaluation of hydroxyapatite reinforced polyethylene composites, British Ceramic Transactions 93 (1994) 91–95.
[9] M. Wang, C.Y. Yue, B. Chua, Production and evaluation of hydroxyapatite reinforced polysulfone for tissue replacement, J. Mater. Sci. Mater. Med. 12 (2001) 821–826.
[10] M. Wang, X.Y. Yang, K.A. Khor, Y. Wang, Preparation, characterisation of bioactive monolayer and functionally graded coatings, J. Mater. Sci. Mater. Med. 10 (1999) 269–273.
[11] R.R. Kumar, M. Wang, P. Ducheyne, Production, Evaluation of hydroxyapatite/tricalcium phosphate functionally graded coating, Bioceramics 13 (2000) 231–234.
[12] M. Wang, H.S. Yong, Production and evaluation of a glass reinforced hydroxyapatite composite, in: Proceedings of the 5th Asian Symposium on Biomedical Materials, Hong Kong, (2001), pp. 101–102.
[13] V. Nelea, C. Morosanu, M. Iliescu, I.N. Mihailescu, thin films grown by RF magnetron sputtering, Surf. Coat. Technol. 173 (2003) 315–322.
[14] H. Li, K.A. Khor, P. Cheang, Young's modulus and fracture toughness determination of high velocity oxy-fuel-sprayed bioceramic coatings, Surf. Coat. Technol. 155 (2002) 21–32.
[15] M. Wang, W. Bonfield, L.L. Hench, Bioglass/high density polyethylene composite as a new soft tissue bonding material, Bioceramics 8 (1995) 383–388.
[16] M. Wang, T. Kokubo, W. Bonfield, A–W glass ceramic reinforced polyethylene composite for medical applications, Bioceramics 9 (1996) 387–390.
[17] S.J. Ding, C.P. Ju, J.H. Chern, Surface reaction of stoichiometric and calcium-deficient hydroxyapatite in simulated body fluid, J. Mater. Sci. Mater. Med. 11 (2000) 183–190.
[18] L. Fu, K.A. Khor, J.P. Lim, Processing, microstructure and mechanical properties of yttria stabilized zirconia reinforced hydroxyapatite coatings, Mater. Sci. Eng. A 316 (2001) 46–51.
[19] M.H. Fathi, F. Azam, Novel hydroxyapatite/tantalum surface coating for metallic dental implant, Mater. Lett. 61 (2007) 1238–1241.
[20] M.H. Fathi, M. Salehi, V. Mortazavi, S.B. Moosavi, The effect of surface characteristics and clinical procedures on corrosion behavior of dental amalgams, Surf. Eng. 17 (2001) 459–464.
[21] C. Daniel, J.J. Clupper, D.C. Mecholsky, D. Greenspan, Bioactivity of tape cast and sintered bioactive glass ceramic in simulated body fluid, Biomaterials 23 (2002) 2599–2606.
[22] P. Sepulveda, J.R. Jones, L.L. Hench, Bioactive sol–gel foams for tissue repair, J. Biomed. Mater. Res. 59 (2002) 340–348.
[23] N. Li, J. Qie, S. Zhu, R. Wang, A new route to prepare macroporous bioactive sol–gel glasses with high mechanical strength, Mater. Lett. 58 (2004) 2747–2750.
[24] M.H. Fathi, M. Kharaziha, Two-step sintering of dense, nanostructural forsterite, Mater. Lett. 63 (2009) 1455–1458.
[25] G. Chen, G.X. Sun, Z.G. Zhu, Study on reaction-processed Al–Cu/α-Al_2O_3 (p) composites, Mater. Sci. Eng. A 265 (1999) 197.
[26] D.M. Liu, T. Troczynski, W.J. Tseng, Sol–gel hydroxyapatite coatings on stainless steel substrates, Biomaterials 22 (2001) 1721–1730.
[27] A. Jillavenkatesa, R.A. Condrate, Sol–gel processing of hydroxyapatite, J. Mater. Sci. 33 (1998) 4111–4119.
[28] M. Kharaziha, M.H. Fathi, Synthesis and characterization of bioactive forsterite nanopowder, Ceram. Int. 35 (2009) 2449–2454.
[29] M.H. Fathi, A. Doost Mohammadi, Preparation and characterization of sol–gel bioactive glass coating for improvement of biocompatibility of human body implant, Mater. Sci. Eng. A. 474 (2008) 128–133.
[30] B.D. Cullity, Elements of XRD diffraction, Addison-Wesley, 1978.
[31] Y.X. Pang, X. Bao, Influence of temperature, ripening time and calcination on the morphology and crystallinity of hydroxyapatite nanoparticles, J. Euro. Ceram. Soc. 23 (2003) 1697–1704.
[32] T. Kokubo, H. Takadama, How useful is SBF in predicting in vivo bone bioactivity, Biomaterials 27 (2006) 2907–2915.
[33] JCPDS Card No. 9-432, 1994.
[34] JCPDS Card No. 34-0189, 1984.